MIMO Radar Ambiguity Optimization Using Frequency-Hopping Waveforms

Chun-Yang Chen and P. P. Vaidyanathan
Dept. of Electrical Engineering, MC 136-93
California Institute of Technology, Pasadena, CA 91125, USA
E-mail: cyc@caltech.edu, ppvnath@systems.caltech.edu

Abstract—Recently, the concept of MIMO (multiple-input-multiple-output) radars has drawn considerable attention. In traditional SIMO (single-input-multiple-output) radar, the transmitters emit coherent waveforms to form a focused beam. In MIMO radar, the transmitters emit orthogonal (or incoherent) waveforms to increase the spatial resolution. These waveforms also affect the range and Doppler resolution which can be characterized by the ambiguity function. In traditional (SIMO) radars, the ambiguity function of the transmitted pulse characterizes the compromise between range and Doppler resolutions. In the MIMO radar, since many transmitting waveforms are involved, their cross-ambiguity functions enter into the signal design problem. In this paper, frequency hopping codes are used to generate these orthogonal MIMO radar waveforms. A new algorithm for designing the frequency hopping codes is proposed. This algorithm makes the energy in the corresponding ambiguity functions evenly spread in the range and angular dimensions. [1]

I. INTRODUCTION

The MIMO (multiple-input multiple-output) radar system allows transmitting orthogonal (or incoherent) waveforms in each of the transmitting antennas. In the traditional SIMO (single-input multiple-output) radar, the system can only transmit scaled versions of a single waveform. It has been shown that the MIMO radar has several advantages over SIMO radar including high spatial resolution [1], excellent interference rejection capability [2], improved parameter identifiability [3], and enhanced flexibility for transmit beampattern design [4].

The waveform design problem in SIMO radar has been well studied. Several waveform design methods have been proposed to meet different resolution requirements. These methods can be found in [8] and the references therein. In the traditional SIMO radar system, the radar receiver uses a matched filter to extract the target signal from thermal noise. Consequently, the resolution of the radar system is determined by the response to a point target in the matched filter output. Such a response can be characterized by a function called the ambiguity function [8]. Recently, San Antonio, et al. [5] have extended the radar ambiguity function to the MIMO radar case. It turns out that the radar waveforms affect not only the range and Doppler resolution but also the angular resolution.

The MIMO radar ambiguity function characterizes the resolutions of the radar system. By choosing different waveforms, we obtain a different MIMO ambiguity function. Therefore the MIMO radar waveform design problem is to choose a set of waveforms which provides a desirable MIMO ambiguity function. Directly optimizing the waveforms requires techniques

such as calculus of variation. In general this can be very hard to solve. Instead of directly designing the waveforms, we can impose some structures on the waveforms and design the parameters of the waveforms. As an example of this idea, the pulse waveforms generated by frequency hopping codes are considered in this paper. These pulses have the advantage of constant modulus. We will show how to optimize the frequency hopping codes to obtain good system resolutions. The corresponding optimization problem can be solved by a simulated annealing algorithm [6].

The rest of the paper is organized as follows. In Section II, the MIMO radar ambiguity function will be briefly reviewed. In Section III, we derive the MIMO radar ambiguity function when the pulse trains are transmitted. In Section IV, we define the frequency hopping pulse waveforms in MIMO radar and derive the corresponding MIMO ambiguity function. In Section V, we formulate the frequency-hopping code optimization problem and show how to solve it. In Section VI, we test the proposed method and compare its ambiguity function with the LFM (linear frequency modulation) waveforms. Finally, Section VII concludes the paper.

II. REVIEW OF THE MIMO RADAR AMBIGUITY FUNCTION

In a SIMO radar system, the radar ambiguity function is defined as [8]

$$|\chi(\tau, \nu)| \triangleq \left| \int_{-\infty}^{\infty} u(t)u^*(t + \tau)e^{j2\pi\nu t} dt \right|, \qquad (1)$$

where $u(t)$ is the radar waveform. This two-dimensional function indicates the matched filter output in the receiver when a delay mismatch τ and a Doppler mismatch ν occur. The value $|\chi(0,0)|$ represents the matched filter output without any mismatch. Therefore, the sharper the function $|\chi(\tau, \nu)|$ around $(0,0)$, the better the Doppler and range resolution.

The idea of radar ambiguity functions has been extended to the MIMO radar by San Antonio et al. [5]. In this section, we will briefly review the definition of MIMO radar ambiguity functions. We will focus only on the linear array case as shown in Fig. 1. We assume the transmitter and the receiver are parallel linear arrays in the same location. The antenna location of the mth transmitting antenna is denoted by $x_{T,m}\frac{\lambda}{2}$ and the antenna location of the nth receiving antenna is denoted by $x_{R,m}\frac{\lambda}{2}$, where λ is the wavelength. The function $u_i(t)$ indicates the radar waveform emitted by the ith transmitter.

Consider a target at (τ, ν, f_s) where τ is the delay corresponding to the target range, ν is the Doppler frequency of the

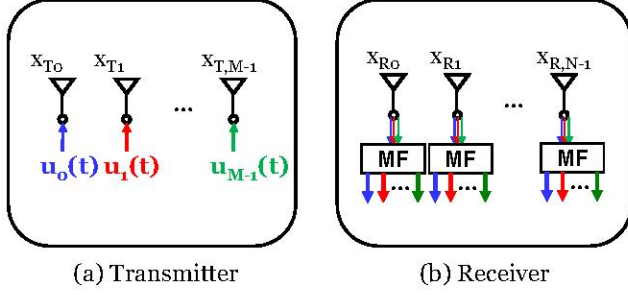(a) Transmitter   (b) Receiver

Fig. 1.   MIMO radar scheme.

target, and f_s is the normalized spatial frequency of the target. The demodulated target response in the nth antenna element is proportional to

$$y_n^{\tau,\nu,f_s}(t) \approx \sum_{m=0}^{M-1} u_m(t-\tau)e^{j2\pi\nu t}e^{j2\pi f_s(x_{T,m}+x_{R,n})},$$

for $n = 0, 1, \cdots, N-1$, where N is the number of receiving antennas, $u_m(t)$ is the radar waveform emitted by the mth antenna and M is the number of transmitting antennas. Define the function

$$\Gamma(\tau,\nu,f_s,\tau',\nu',f_s') = \sum_{n=0}^{N-1} \int_{-\infty}^{\infty} y_n^{\tau,\nu,f_s}(t) \cdot (y_n^{\tau',\nu',f_s'})^*(t)dt.$$

We would like this to be large when $(\tau,\nu,f_s) = (\tau',\nu',f_s')$ and small otherwise. We call this the overall matched filter response. It can be simplified to the form

$$\begin{aligned}
&\Gamma(\tau,\nu,f_s,\tau',\nu',f_s') \\
&= \left(\sum_{n=0}^{N-1} e^{j2\pi(f_s-f_s')x_{T,n}} \right) \cdot \\
&\quad \left(\sum_{m=0}^{M-1}\sum_{m'=0}^{M-1} \int_{-\infty}^{\infty} u_m(t-\tau)u_{m'}^*(t-\tau') \right. \\
&\quad \left. e^{j2\pi(\nu-\nu')t}dt \cdot e^{j2\pi(f_s x_{T,m}-f_s'x_{T,m'})} \right)
\end{aligned}$$

The first part in the right hand side of the equation represents the spatial processing in the receiver, and it is not affected by the waveforms $\{u_m(t)\}$. The second part in the right hand side of the equation indicates how the waveforms $\{u_m(t)\}$ affect the spatial, Doppler and range resolutions of the radar system. Therefore, we define the **MIMO radar ambiguity function** as

$$\begin{aligned}
&\chi(\tau,\nu,f_s,f_s') \triangleq \\
&\sum_{m=0}^{M-1}\sum_{m=0}^{M-1} \chi_{m,m'}(\tau,\nu)e^{j2\pi(f_s x_{T,m}-f_s'x_{T,m'})}, \quad (2)
\end{aligned}$$

where

$$\chi_{m,m'}(\tau,\nu) \triangleq \int_{-\infty}^{\infty} u_m(t)u_{m'}^*(t+\tau)e^{j2\pi\nu t}dt. \quad (3)$$

Note that the MIMO radar ambiguity function can not be expressed as a function of the difference of the spatial

frequencies, namely $f_s - f_s'$. Therefore, we need both the target spatial frequency f_s and the assumed spatial frequency f_s' to represent the spatial mismatch. We call the function $\chi_{m,m'}(\tau,\nu)$ the **cross ambiguity function** because it is similar to the SIMO ambiguity function defined in (1) except it involves two waveforms $u_m(t)$ and $u_{m'}(t)$. Fixing τ and ν in (2), one can view the ambiguity function as a scaled two-dimensional Fourier transform of the cross ambiguity function $\chi_{m,m'}(\tau,\nu)$ on the parameters m and m'. The value $|\chi(0,0,f_s,f_s)|$ represents the matched filter output without mismatch. Therefore, the sharper the function $|\chi(\tau,\nu,f_s,f_s')|$ around the line $\{(0,0,f_s,f_s)\}$ (Sec. V), the better the radar system resolution.

III. PULSE MIMO RADAR AMBIGUITY FUNCTION

In this section, we derive the MIMO radar ambiguity function for the case when the waveform $u_m(t)$ consists of the shifted versions of a shorter waveform $\phi_m(t)$. In this case, the pulse design problem becomes choosing the waveform $\phi_m(t)$ to obtain a good MIMO ambiguity function $\chi(\tau,\nu,f_s,f_s')$. Therefore, it is important to study the relation between the MIMO ambiguity function and the pulse $\phi_m(t)$. Since modulation and scalar multiplication will not change the shape of the ambiguity function, for convenience, we write the transmitted signals as

$$u_m(t) = \sum_{l=0}^{L-1} \phi_m(t-T_l) \quad (4)$$

Note that the duration of $\phi_m(t)$, namely T_ϕ, is small enough such that $T_\phi \ll \min(|T_l - T_{l'}|)$. To obtain the relation between $\phi_m(t)$ and the MIMO ambiguity function $\chi(\tau,\nu,f_s,f_s')$, we first derive the cross ambiguity function. Using (3) and (4) and changing variables, the cross ambiguity function can be expressed as

$$\begin{aligned}
&\chi_{m,m'}(\tau,\nu) = \\
&\sum_{l'=0}^{L-1}\sum_{l=0}^{L-1} \int_{-\infty}^{\infty} \phi_m(t)\phi_{m'}^*(t+T_l-T_{l'}+\tau)e^{j2\pi\nu(t+T_l)}dt \\
&= \sum_{l'=0}^{L-1}\sum_{l=0}^{L-1} \chi_{m,m'}^\phi(\tau+T_l-T_{l'},\nu)e^{j2\pi\nu T_l}, \quad (5)
\end{aligned}$$

where $\chi_{m,m'}^\phi(\tau,\nu)$ is defined as the cross ambiguity function of the pulses $\phi_m(t)$ and $\phi_{m'}(t)$, that is,

$$\chi_{m,m'}^\phi(\tau,\nu) = \int_0^{T_\phi} \phi_m(t)\phi_{m'}^*(t+\tau)e^{j2\pi\nu t}dt.$$

We assume that the Doppler frequency ν and the support of pulse T_ϕ are both small enough such that $T_\phi\nu \approx 0$. So the above the equation becomes

$$\chi_{m,m'}^\phi(\tau,\nu) \approx \int_0^{T_\phi} \phi_m(t)\phi_{m'}^*(t+\tau)dt \triangleq r_{m,m'}^\phi(\tau), \quad (6)$$

where $r_{m,m'}^\phi(\tau)$ is the cross correlation between $\phi_m(t)$ and $\phi_{m'}(t)$. Thus, the cross ambiguity function reduces to the cross

correlation function and it is no longer a function of Doppler frequency ν. Substituting the above result into (5), we obtain

$$\chi_{m,m'}(\tau, \nu) \approx \sum_{l'=0}^{L-1} \sum_{l=0}^{L-1} r_{m,m'}^{\phi}(\tau + T_l - T_{l'}) e^{j2\pi\nu T_l} \qquad (7)$$

For values of the delay τ satisfying $|\tau| < \min(|T_l - T_{l'}|) - T_{\phi}$, the shifted correlation function satisfies

$$r_{m,m'}^{\phi}(\tau + T_l - T_{l'}) =$$
$$\int_0^{T_{\phi}} \phi_m(\tau) \phi_{m'}^*(t + \tau + T_l - T_{l'}) dt = 0,$$

when $l \neq l'$. For $|\tau| \geq \min(|T_l - T_{l'}|) - T_{\phi}$, the response in the ambiguity function is created by the second trip echoes. This ambiguity is called range folding. Such ambiguity can be resolved by using a different pulse repetition frequency (PRF) from time to time. We will not address this ambiguity in this paper. We will focus on the ambiguity function only when $|\tau| < \min(|T_l - T_{l'}|) - T_{\phi}$. In this case, we have

$$\chi_{m,m'}(\tau, \nu) \approx r_{m,m'}^{\phi}(\tau) \sum_{l=0}^{L-1} e^{j2\pi\nu T_l}.$$

Notice that the Doppler processing is separable from the correlation function. This is because of the assumption that the duration of the pulses T_{ϕ} and the Doppler frequency ν are small enough so that $\nu T_{\phi} \approx 0$. This implies that the choice of the waveforms $\{\phi_m(t)\}$ does not affect the Doppler resolution. Using the definition of MIMO ambiguity function (2), we have

$$\chi(\tau, \nu, f_s, f_s') =$$
$$\sum_{m=0}^{M-1} \sum_{m'=0}^{M-1} r_{m,m'}^{\phi}(\tau) e^{j2\pi(f_s x_{T,m} - f_s' x_{T,m'})} \cdot \sum_{l=0}^{L-1} e^{j2\pi\nu T_l},$$

for $|\tau| < \min(|T_l - T_{l'}|) - T_{\phi}$.

The preceding analysis clearly shows how the problem of waveform design should be approached. The MIMO ambiguity function depends on the cross correlation functions $r_{m,m'}^{\phi}(\tau)$. Also, the pulses $\{\phi_m(t)\}$ only affect the range and spatial resolution. They do not affect the Doppler resolution. Therefore, to obtain a sharp ambiguity function, we should design the pulses $\{\phi_m(t)\}$ such that the function

$$\Omega(\tau, f_s, f_s') \triangleq \sum_{m=0}^{M-1} \sum_{m'=0}^{M-1} r_{m,m'}^{\phi}(\tau) e^{j2\pi(f_s x_{T,m} - f_s' x_{T,m'})} \qquad (8)$$

is sharp around the line $\{(\tau, f_s, f_s') | \tau = 0, f_s = f_s'\}$. For $M = 1$, the signal design problem reduces to the special case of the SIMO radar. In this case, equation (8) reduces to the autocorrelation function

$$\Omega(\tau, f_s, f_s') = r_{0,0}^{\phi}(\tau).$$

Thus in the SIMO radar case, the signal design problem is to generate a pulse with a sharp autocorrelation. The linear frequency modulation (LFM) signal is an example which has a sharp autocorrelation [8]. Besides its sharp autocorrelation function, the LFM pulse can be conveniently generated and it has constant modulus. These reasons make the LFM signal a very good candidate in a pulse repetition radar system. For the

MIMO radar case which satisfies $M > 1$, we need to consider not only the autocorrelation functions but also the cross correlation functions between pulses such that $\Omega(\tau, f_s, f_s')$ can be sharp.

IV. FREQUENCY HOPPING PULSES

Instead of directly designing the pulses, we can impose some structures on the pulses and design the parameters of the pulses. As an example of this idea, we now consider the pulse generated by frequency hopping codes. In this section, we derive the MIMO radar ambiguity function of the frequency hopping pulses. These pulses have the advantage of constant modulus. The frequency hopping pulses can be expressed as

$$\phi_m(t) = \sum_{q=0}^{Q-1} e^{j2\pi c_{m,q}\Delta f t} 1_{[0,\Delta t)}(t - q\Delta t), \qquad (9)$$

where

$$1_{[0,\Delta t)}(t) \triangleq \begin{cases} 1, & t \in [0, \Delta t) \\ 0, & \text{otherwise,} \end{cases}$$

$c_{m,q} \in \{0, 1, \cdots, K-1\}$ is the frequency hopping code, and Q is the length of the code. The duration of the pulse is $T_{\phi} = Q\Delta t$, and the bandwidth of the pulses is approximately

$$(K-1)\Delta f + \frac{1}{\Delta t}.$$

To maintain the orthogonality, the code $\{c_{m,q}\}$ satisfies

$$c_{m,q} \neq c_{m',q}, \text{ for } m \neq m', \forall q \qquad (10)$$
$$\Delta t \Delta f = 1.$$

Now instead of directly designing the pulses $\phi_m(t)$, the signal design problem becomes designing the code $c_{m,q}$ for $m = 0, 1, \cdots, M-1$ and $q = 0, 1, \cdots, Q-1$. Recall that our goal is to design the transmitted signals such that the function $\Omega(\tau, f_s, f_s')$ in (8) is sharp (as explained in Sec. V). So, we are interested in the expression for the function $\Omega(\tau, f_s, f_s')$ in terms of $\{c_{m,q}\}$. To compute the function $\Omega(\tau, f_s, f_s')$, we first compute the cross correlation function $r_{m,m}^{\phi}(\tau)$. By using (9) and (6), it can be expressed as

$$r_{m,m'}^{\phi}(\tau) = \qquad (11)$$
$$\sum_{q=0}^{Q-1} \sum_{q'=0}^{Q-1} \chi^{\text{rect}}\big(\tau - (q' - q)\Delta t, (c_{m,q} - c_{m',q'})\Delta f\big)$$
$$\cdot e^{j2\pi\Delta f(c_{m,q} - c_{m',q'})q\Delta t} e^{j2\pi\Delta f c_{m',p'}\tau},$$

where $\chi^{\text{rect}}(\tau, \nu)$ is the SIMO ambiguity function of the rectangular pulse $1_{[0,\Delta t)}(t)$, given by

$$\chi^{\text{rect}}(\tau, \nu) \triangleq \int_0^{\Delta t} 1_{[0,\Delta t)}(t) 1_{[0,\Delta t)}(t + \tau) e^{j2\pi\nu t} dt \qquad (12)$$
$$= \begin{cases} \frac{\Delta t - |\tau|}{\Delta t} \text{sinc}\left(\nu(\Delta t - |\tau|)\right) e^{j\pi\nu(\tau + \Delta t)}, \text{if } |\tau| < \Delta t \\ 0, \text{otherwise.} \end{cases}$$

Substituting (11) into (8), we obtain

$$\Omega(\tau, f_s, f_s') =$$
$$\sum_{m,m'=0}^{M-1} \sum_{q,q'=0}^{Q-1} \chi^{\text{rect}}\big(\tau - (q' - q)\Delta t, (c_{m,q} - c_{m',q'})\Delta f\big)$$
$$\cdot e^{j2\pi\Delta f(c_{m,q} - c_{m',q'})q\Delta t} e^{j2\pi\Delta f c_{m',q'}\tau} e^{j2\pi(f_s x_{T,m} - f_s' x_{T,m'})}.$$

Define $\tau = k\Delta t + \eta$, where $|\eta| < \Delta t$. By using the fact that $\chi^{\mathrm{rect}}(\tau, \nu) = 0$ when $|\tau| > \Delta t$, the above equation can be further simplified as

$$\Omega(k\Delta t + \eta, f_s, f_s') = \tag{13}$$
$$\sum_{m,m'=0}^{M-1} \sum_{q=0}^{Q-1} \chi^{\mathrm{rect}}\big(\eta, (c_{m,q} - c_{m',q+k})\Delta f\big)$$
$$\cdot e^{j2\pi\Delta f c_{m',q+k}(k\Delta t + \eta)} e^{j2\pi\Delta f(c_{m,q} - c_{m',q+k})q\Delta t}$$
$$\cdot e^{j2\pi(f_s x_{T,m} - f_s' x_{T,m'})}.$$

The next step is to choose the frequency hopping code $\{c_{m,q}\}$ such that the function $\Omega(\tau, f_s, f_s')$ is sharp around $\{0, f_s, f_s'\}$. We will discuss this in the following section.

V. OPTIMIZATION OF THE FREQUENCY HOPPING CODES

In this section, we introduce an algorithm to search for frequency hopping codes which generate good MIMO ambiguity functions. By using (8) and the orthogonality of the waveforms, we have

$$\Omega(0, f_s, f_s) = \sum_{m,m'=0}^{M-1} \delta_{m,m'} e^{j2\pi f_s(x_{T,m} - x_{T,m'})} = M.$$

So, we know that the function $\Omega(\tau, f_s, f_s)$ is a constant along the line $\{0, f_s, f_s\}$, no matter what codes are chosen. To obtain good system resolutions, we need to eliminate the peaks in $|\Omega(\tau, f_s, f_s')|$ which are not on the line $\{0, f_s, f_s\}$. This can be done by imposing a cost function which puts penalties on these peak values. This forces the energy of the function $\Omega(\tau, f_s, f_s')$ to be evenly spread in the delay and angular dimensions. As an example of this, we minimize the p-norm of the function $\Omega(\tau, f_s, f_s')$. The corresponding optimization problem can be expressed as

$$\min_{\mathbf{C}} f_p(\mathbf{C}) \tag{14}$$
$$\text{subject to} \quad \mathbf{C} \in \{0, 1, \cdots, K-1\}^{MQ}$$
$$c_{m,q} \neq c_{m',q}, \text{ for } m \neq m',$$

where

$$f_p(\mathbf{C}) \triangleq \int_{-\infty}^{\infty} \int_0^1 \int_0^1 |\Omega(\tau, f_s, f_s')|^p df_s df_s' d\tau. \tag{15}$$

Note that a greater p imposes more penalty on the higher peaks. The feasible set of this problem is a discrete set. It is known that simulated annealing algorithm is very suitable for solving this kind of problems [6]. The simulated annealing algorithm runs a Markov chain Monte Carlo (MCMC) sampling on the discrete feasible set [7]. The transition probability of the Markov chain can be chosen so that the equilibrium of the Markov chain is

$$\pi_T(\mathbf{C}) = \frac{1}{Z_T} \exp(\frac{-f_p(\mathbf{C})}{T}), \text{ where}$$
$$Z_T = \sum_{\mathbf{C}} \exp(\frac{-f_p(\mathbf{C})}{T}). \tag{16}$$

Here T is a parameter called temperature. By running the MCMC and gradually decreasing the temperature T, the generated sample $\mathbf{C}$ will have a high probability to have

a small cost function output [6]. In our case, the transition probability from state $\mathbf{C}$ to $\mathbf{C}'$ is chosen as

$$p(\mathbf{C}, \mathbf{C}') =$$
$$\begin{cases} \frac{1}{d} \min(1, \exp(\frac{f_p(\mathbf{C}) - f_p(\mathbf{C}')}{T})), & \text{if } \mathbf{C}' \sim \mathbf{C} \\ 1 - \frac{1}{d} \sum_{\mathbf{C}'' \sim \mathbf{C}} \min(1, \exp(\frac{f_p(\mathbf{C}) - f_p(\mathbf{C}'')}{T})), & \text{if } \mathbf{C}' = \mathbf{C} \\ 0, & \text{otherwise,} \end{cases}$$

where $\mathbf{C}' \sim \mathbf{C}$ denotes that $\mathbf{C}'$ and $\mathbf{C}$ differ in exactly one element, and d denotes $\big|\{\mathbf{C}' | \mathbf{C}' \sim \mathbf{C}\}\big|$. It can be shown that the chosen transition probabilities result in the desire equilibrium in (16).

VI. DESIGN EXAMPLES

In this section, we present a design example using the proposed method. In this example, we consider a uniform linear transmitting array. The number of transmitted waveforms M equals 4. The length of the frequency hopping code Q equals 10. The number of frequencies K equals 15. Without loss of generality, we normalize the pulse duration T_ϕ to be unity. By using (10), we obtain that the time-bandwidth product $K\Delta f Q\Delta t = 150$. Fig. 2 shows the real parts of the waveforms generated by the proposed algorithm. For comparison Fig. 3
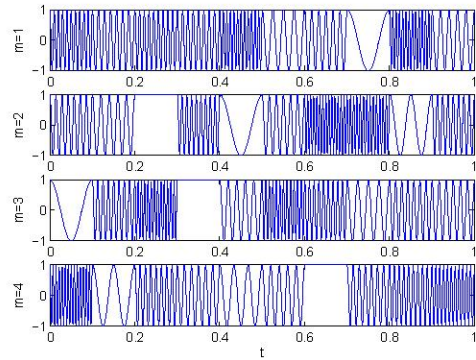

Fig. 2. Real parts of the waveforms obtained by the proposed method.

shows the real parts of orthogonal LFM waveforms. In this example, these LFM waveforms have the form

$$\phi_m(t) = \exp(j2\pi f_{m,0} t + j\pi k t^2),$$

where $k = 100$, $f_{0,0} = 0$, $f_{1,0} = \frac{50}{3}$, $f_{2,0} = \frac{100}{3}$, and $f_{3,0} = 50$. By choosing different initial frequencies, these LFM waveforms can be made orthogonal. These parameters are chosen so that these LFM waveforms occupies the same time duration and bandwidth as the waveforms generated by the proposed method. Fig. 4 shows a result of comparing the functions $|\Omega(\tau, f_s, f_s')|$. We take samples from the function $|\Omega(\tau, f_s, f_s')|$ and sort these samples in descending order. Fig. 4 shows the first ten percent of these samples. We have normalized the highest peak to 0 dB. In other words, this figure shows the percentage of samples of $|\Omega(\tau, f_s, f_s')|$ equal to a fixed amplitude β, for various β. The results of the proposed method, randomly generated frequency hopping codes, and the
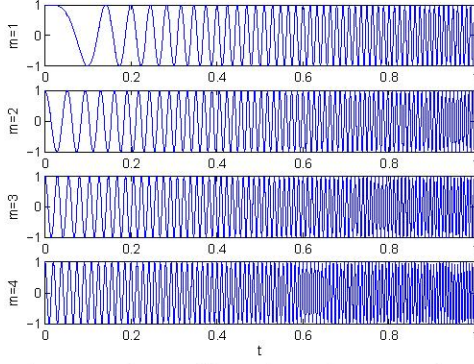
Fig. 3.   Real parts of the orthogonal LFM waveforms.

Fig. 5.   Cross correlation functions $r^{\phi}_{m,m'}(\tau)$ of the waveforms generated by the proposed method.

LFM waveforms are compared in the figure. One can see that the proposed frequency hopping signals yield fewest undesired peaks among all the waveforms. The video which shows the entire function $|\Omega(\tau, f_s, f'_s)|$ (a plot in (f_s, f'_s) plane as a function of time τ) can be downloaded from [9]. Fig. 5 shows

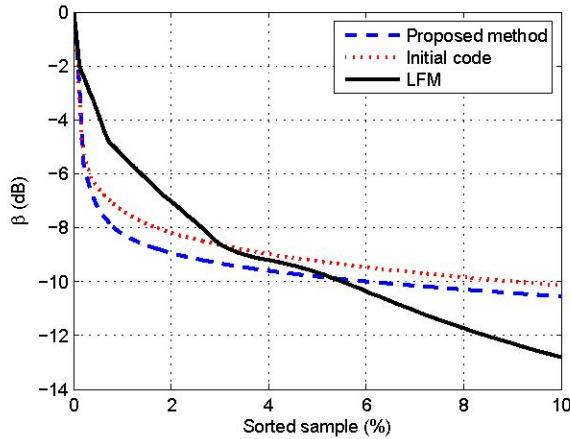Fig. 6.   Cross correlation functions $r^{\phi}_{m,m'}(\tau)$ of the LFM waveforms.

Fig. 4.   Sorted samples of $|\Omega(\tau, f_s, f'_s)|$.

the cross correlation functions $r^{\phi}_{m,m'}(\tau)$ of the waveforms generated by the proposed algorithm. Fig. 6 shows the cross correlation functions $r^{\phi}_{m,m'}(\tau)$ of the LFM waveforms. One can observe that for the proposed waveforms, the correlation functions $r^{\phi}_{m,m'}(\tau)$ equal to unity when $m = m'$ and $\tau = 0$. Except at these points, the correlation functions are small everywhere. However, for the LFM waveforms, the correlation functions have several extraneous peaks. These peaks also form peaks in the ambiguity function.

VII. CONCLUSIONS

In this paper, we have introduced a waveform design method for MIMO radars. This method is applicable to the case where the transmitted waveforms are orthogonal and consist of multiple shifted narrow pulses. The proposed method applies the simulated annealing algorithm to search for the frequency hopping codes which minimize the p-norm of the ambiguity
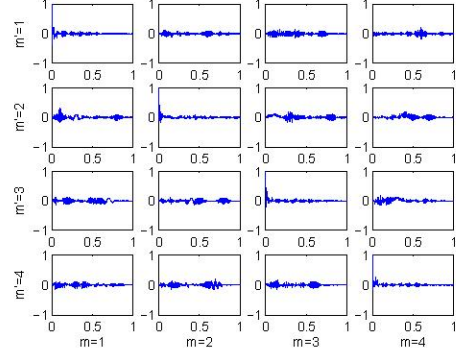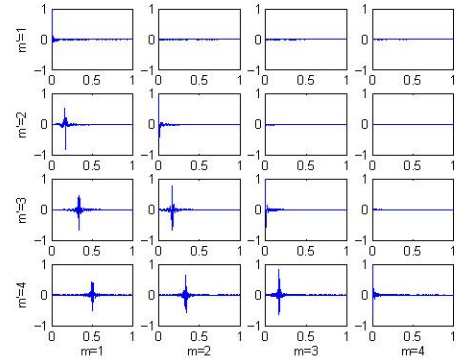
function. The numerical examples show that the waveforms generated by this method provide better angular and range resolutions than the LFM waveforms which have often been used in the traditional SIMO radar systems. In this paper, we have presented the results only for the case of linear arrays. Nevertheless it is possible to further generalize these results for multi-dimensional arrays.

REFERENCES

[1] D. W. Bliss and K. W. Forsythe, "Multiple-Input Multiple-Output (MIMO) Radar and Imaging: Degrees of Freedom and Resolution," *Proc. 37th IEEE Asilomar Conf. on Signals, Systems, and Computers,* vol. 1, pp. 54-59, Nov. 2003.
[2] Chun-Yang Chen and P. P. Vaidyanathan, "MIMO Radar Space-Time Adaptive Processing Using Prolate Spheroidal Wave Functions," *IEEE Trans. on Signal Processing*, to appear.
[3] J. Li, P. Stoica, L. Xu, and W. Roberts, "On Parameter Identifiability of MIMO Radar," *IEEE Signal Processing Letters*, to appear.
[4] P. Stoica, J. Li, and Y. Xie, "On Probing Signal Design For MIMO Radar," *IEEE Trans. on Signal Processing* Volume 55, Issue 8, Aug. 2007.
[5] G. San Antonio, D. R. Fuhrmann, and F. C. Robey, "MIMO Radar Ambiguity Functions," *IEEE Journal of Selected Topics in Signal Processing,* vol. 1, pp. 167-177, Jun. 2007.
[6] S. Kirkpatrick, C. D. Gelatt and M. P. Vecchi, "Optimization by Simulated Annealing," *Science,* vol. 220, no. 4598, pp. 671-680, 1983.
[7] N. Metropolis, A.W. Rosenbluth, M.N. Rosenbluth, A.H. Teller, and E. Teller. "Equations of State Calculations by Fast Computing Machines," Journal of Chemical Physics, vol. 21, no. 6, pp. 1087-1092, 1953.
[8] N. Levanon and E. Mozeson, *Radar Signals,* Wiley-IEEE Press, 2004.
[9] http://www.systems.caltech.edu/cyc/amb-fun.htm